Original Article

Iodine-based extracellular volume for evaluating myocardial status in patients undergoing percutaneous coronary intervention for acute myocardial infarction by using dual-layer spectral detector computed tomography: a comparison study with magnetic resonance

Jing Liang[1#], Hui Li[1#], Jun Xie[2], Hongming Yu[1], Wenping Chen[1], Kejie Yin[1], Xingbiao Chen[3], Zhihong Sheng[3], Xin Zhang[1], Dan Mu[1]

[1]Department of Radiology, Nanjing Drum Tower Hospital, The Affiliated Hospital of Nanjing University Medical School, Nanjing, China; [2]Department of Cardiology, Nanjing Drum Tower Hospital, The Affiliated Hospital of Nanjing University Medical School, Nanjing, China; [3]Clinical Science, Philips Healthcare, Shanghai, China

Contributions: (I) Conception and design: J Liang, H Li; (II) Administrative support: M Dan, X Zhang; (III) Provision of study materials or patients: H Yu, J Xie, W Chen; (IV) Collection and assembly of data: J Liang, K Yin; (V) Data analysis and interpretation: X Chen, Z Sheng; (VI) Manuscript writing: All authors; (VII) Final approval of manuscript: All authors.

[#]These authors contributed equally to this work.

Correspondence to: Xin Zhang. Department of Radiology, Nanjing Drum Tower Hospital, The Affiliated Hospital of Nanjing University Medical School, 321 Zhongshan Road, Nanjing 210008, China. Email: zhangxin@njglyy.com; Dan Mu. Department of Radiology, Nanjing Drum Tower Hospital, The Affiliated Hospital of Nanjing University Medical School, 321 Zhongshan Road, Nanjing 210008, China. Email: mudan118@126.com.

Background: The myocardial status of patients who undergo percutaneous coronary intervention (PCI) must be evaluated accurately to enable treatment plans to be made for potential complications such as abrupt vessel closure, stent deformation, and myocardial chronic ischemia. This study examined the modality and clinical feasibility of iodine-based extracellular volume (ECV) assessment of the myocardium versus cardiovascular magnetic resonance (CMR) imaging in patients undergoing PCI.

Methods: In all, 21 patients who underwent PCI were prospectively enrolled in the study. All patients underwent follow-up cardiac dual-layer spectral detector computed tomography (SDCT) and CMR imaging after PCI. Myocardial ECV was quantified by either computed tomography (ECV_{CT}) or magnetic resonance (ECV_{MR}) using iodine or T_1-weighted mapping, respectively. The quality of SDCT and CMR images was independently assessed by two radiologists using a 4-point scale (1= poor and 4= excellent). Any patient with an image quality (IQ) score <2 was excluded. Consistency between radiologists was evaluated using intraclass correlation coefficients (ICC). Correlations between ECV_{CT} and ECV_{MR} values were analyzed using Pearson's test, and consistency was analyzed with Bland–Altman plots.

Results: Nineteen of 21 patients completed both cardiac CT and CMR examinations, while three patients were excluded after IQ assessment (two with poor CMR IQ; one with a discontinuous coronary artery on CT images). The mean (±SD) IQ scores for CT and CMR images were 3.81±0.40 and 3.25±0.58, respectively, and interobserver agreement was good (ICC =0.93 and 0.92 for CT and CMR, respectively). The mean (±SD) ECV_{CT} and ECV_{MR} values were 35.93%±9.73% and 33.89%±7.51%, respectively, with good correlation (r=0.79, P<0.001). Bland–Altman analysis showed a difference of 2.04% (95% CI: –9.56%, 13.64%) between the ECV_{CT} and ECV_{MR} values.

Conclusions: There is high correlation between iodine-based ECV_{CT} and ECV_{MR} values, which indicates

that ECV_{CT} is clinically feasible for evaluating the status of myocardial recovery in patients undergoing PCI.

Keywords: Extracellular volume (ECV); magnetic resonance; myocardial infarction; percutaneous coronary intervention (PCI); spectral detector computed tomography (SDCT)

Submitted Nov 13, 2021. Accepted for publication May 19, 2022.
doi: 10.21037/qims-21-1103
View this article at: https://dx.doi.org/10.21037/qims-21-1103

Introduction

Coronary artery disease (CAD) can cause a heart attack or stroke by decreasing blood flow through the arteries (1). Percutaneous coronary intervention (PCI) has been successfully used to treat and improve CAD symptoms in patients, and is less invasive, lower cost, and associated with shorter hospital stays than is surgical intervention (2). However, there are various perioperative complications that can affect the myocardial prognosis after PCI, including coronary perforation, abrupt vessel closure, stent deformation, wire fracture, and, in particular, chronic myocardial ischemia caused by in-stent restenosis (3). It is therefore critical to accurately assess myocardial status postoperatively to support the development of treatment plans for such complications.

Previous studies have demonstrated that myocardial extracellular volume (ECV) based on late gadolinium-enhanced cardiovascular magnetic resonance (CMR) imaging can quantitatively reflect myocardial infarction (4). It has also been proven to be an effective quantitative parameter for predicting long-term cardiac functional recovery and adverse left ventricular remodeling events (5,6). However, ECV may be difficult to obtain in patients who have undergone PCI, due to poor-quality CMR images resulting from the long scanning time. Currently, cardiac coronary computed tomography angiography (CCTA) is widely used to evaluate arterial stenosis before and after PCI (7). Studies have revealed that ECV can also be calculated using data obtained from late iodine-enhanced (LIE) scans after CCTA to assess the myocardial condition (8,9). The ECV is calculated using the difference in the myocardial computed tomography (CT) values obtained before and after contrast enhancement scanning. However, the accuracy of the results can be affected by the position registration of the myocardium between the pre- and post-enhancement scans (8).

The emergence of spectral CT has made it possible to perform material decomposition with high- and low-energy X-rays, which enables iodine quantitation and improves tissue differentiation in the myocardium (10-12). Dual-layer spectral detector CT (SDCT) permits the simultaneous detection of high- and low-energy X-rays. The detector's unique design allows for spectral reconstruction in the projection domain and enables spectral data acquisition for every scan. One important application of this technique is the calculation of myocardial ECV values. To overcome registration issues in calculating the myocardial ECV, an iodine-based method that only requires data from the LIE phase has been proposed (13). The present study investigated the feasibility of using iodine-based ECV obtained from SDCT to evaluate the myocardium in patients after PCI. We present the following article in accordance with the STARD reporting checklist (available at https://qims.amegroups.com/article/view/10.21037/qims-21-1103/rc).

Methods

Study population

The study was conducted in accordance with the Declaration of Helsinki (as revised in 2013). This single-center prospective cohort study was approved by the Institutional Review Board of Nanjing Drum Tower Hospital (No. 2018-046-01), and written informed consent was obtained from all participants.

Between September 2019 and June 2020, 21 patients with coronary heart disease who underwent PCI for the treatment of acute myocardial infarction (AMI) in Nanjing Drum Tower Hospital were prospectively enrolled in the study (*Figure 1*). To be eligible for inclusion in the study, patients needed to have: (I) a diagnosis of AMI based on biochemistry and electrocardiogram (ECG) changes within 12 hours after the onset of clinical symptoms, such as angina; (II) at least one unobstructed coronary artery (to permit comparison between the infarcted and normal myocardium); and (III) postoperative New York

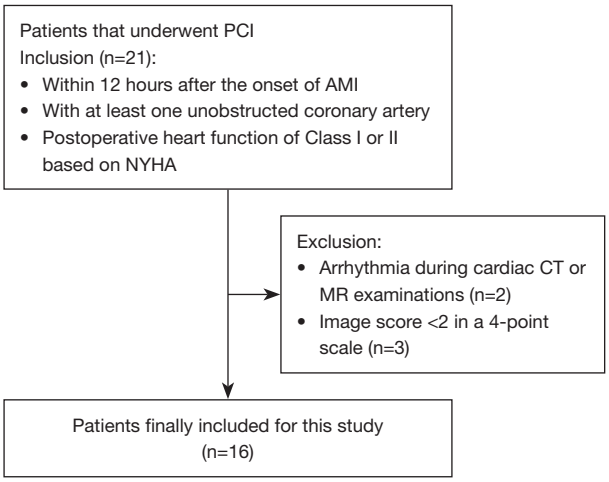

Figure 1 Study flowchart. PCI, percutaneous coronary intervention; AMI, acute myocardial infarction; NYHA, New York Heart Association; CT, computed tomography; MR, magnetic resonance.

Heart Association (NYHA) functional class I or II. The diagnostic criteria for AMI in this study were a rise and/or fall in serially tested cardiac biomarkers (preferably cardiac troponins) with at least one value above the 99th percentile of the upper reference limit, in addition to symptoms of ischemia, new changes on ECG, imaging evidence of a new loss of viable myocardium or new regional wall motion abnormalities, or the identification of an intracoronary thrombus. Patients were excluded from the study if they had undergone coronary artery bypass grafting, had arrhythmia during cardiac CT or CMR follow-up examinations, or had cardiomyopathy (e.g., dilated cardiomyopathy, myocardial hypertrophy), valvular heart disease (e.g., mitral insufficiency, severe tricuspid regurgitation), hemodynamic instability, renal insufficiency, or contraindications for MR or CT. Patients with SDCT and CMR images of poor quality, which was defined as an image quality (IQ) score <2, were also excluded (IQ was assessed using a 4-point scale, on which 1= poor and 4= excellent) (1). Follow-up CMR and CT examinations were performed within 24 hours of each other at 12 weeks after PCI. Hematocrit (Hct) levels were measured in venous blood samples obtained within 1 hour before each examination.

MRI protocol

Participants underwent CMR examination on a 3-T MR scanner (Ingenia CX 3.0T; Philips Healthcare, Best, The Netherlands) with a 32-element phased-array body coil. To ensure good IQ and avoid motion artifacts, CMR images were collected with the assistance of ECG and respiratory-gated technology.

The CMR parameters were as follows:

- Steady state free-precession sequence: repetition time (TR), 3.2 ms; echo time (TE), 1.6 ms; flip angle, 45°; slice thickness, 8 mm.
- T_2-weighted short-tau triple inversion recovery sequence: TR, 2 R-R intervals; TE, 90 ms; flip angle, 90°; slice thickness, 8 mm.
- Breath-hold Modified Look-Locker inversion recovery (MOLLI) sequence: TR, 8.0 ms; TE, 3.5 ms; flip angle, 45°; slice thickness, 8 mm; in-plane resolution, 2.78×2.92×10.0 mm^3.

To obtain T_1-weighted maps of the myocardium and to calculate ECV, T_1-weighted mapping was performed using the ECG-gated MOLLI sequence before and at 10 minutes after intravenous administration of 0.2 mmol/kg MR contrast agent (Magnevist; Bayer Healthcare, Berlin, Germany) in three short-axis slices, including at the basal, midventricular, and apical levels.

CT protocol

All CT examinations were performed using an SDCT (IQon Spectral CT; Philips, Best, The Netherlands). Patients with sinus tachycardia were administered metoprolol tartrate tablets (12.5 mg, sublingual; AstraZeneca, London, UK). To ensure that the whole heart was scanned, the scanning range was set from 1 cm below the carina to the upper boundary of the diaphragm. First, CCTA was performed with iodine contrast (Ioversol; 350 mg/mL iodine; Hengrui, Jiangsu, China), administered at a dose of 0.9–1.0 mg/kg in each patient at an injection flow rate of 4.5–5.0 mL/s. At 8 minutes after the contrast injection, LIE of a prospective ECG-triggered axial scan, with the mid-diastolic phase of the left ventricle (LV) selected as the trigger time point, was performed. The parameters were set as follows: tube voltage, 120 kV; tube current, 150 mA; collimator width, 64×0.625 mm; tube rotation speed, 0.27 s/cycle; reconstruction field of view, 350 mm. The radiation dose of the LIE phase scan was expressed as the effective dose (ED; mSv) and was calculated using the following equation (14):

$$\mathrm{ED}(\mathrm{mSv}) = \mathrm{DLP} \times 0.14 \quad [1]$$

where DLP (mGy·cm) is the dose–length product.

Image analysis

All CMR and CT images were independently reviewed by two radiologists (WC and DM, with 5 and 8 years' experience in cardiovascular imaging, respectively), who were blinded to the participants' clinical histories and other diagnostic test results. In cases of discrepancy, a decision was reached by consensus.

IQ evaluation

The IQ of both CMR and CT images was evaluated. For CMR images, the delineation of the myocardium and the luminal margin was considered, as well as the presence of motion, flow, and pulsation artifacts. For CT images, due to the high scanning speed, attention was paid to the continuity of the coronary arteries after reconstruction. A 4-point scale was used to grade IQ, as follows: the score of 1 indicated poor quality: the myocardial margin was not identifiable. A score of 2 indicated adequate quality: the myocardial margin was visible, but the compositional substructure was partially obscured. A score of 3 indicated good quality: motion and flow artifacts were minimal, and the myocardial margin was clearly defined. A score of 4 indicated excellent quality: no artifacts were seen, and the myocardial margin were depicted in detail. Images with an IQ score <2 were excluded from the analysis (15).

Calculation of CT- and CMR-based ECV

The myocardial ECV was quantified by either CT (ECV_{CT}) or MR (ECV_{MR}).

Iodine mapping was derived from spectral-based images generated by SDCT using a commercially available three-dimensional workstation (IntelliSpacePortal version 10; Philips Healthcare) (16,17). After the iodine map had been generated, the short-axis plane of the LV was reconstructed in accordance with the positional and geometric parameters of T_1-weighted mapping for further analysis. The myocardium was then manually divided into 16 segments according to the American Heart Association (AHA) model, and the ECV_{CT} map was generated (*Figure 2*). To obtain the iodine value of the blood pool, a region of interest of at least 150 mm^2 was placed in the LV cavity. The ECV_{CT} (%) value of each segment was calculated using the following equation, taking Hct into consideration:

$$ECV=(1-Hct)\times Iodine_{myocardium}/Iodine_{blood\ pool} \quad [2]$$

ECV_{MR} was calculated using pre- and post-enhancement T_1-weighted mapping with cvi42 version 5.1 software (Circle Cardiovascular Imaging, Calgary, Canada). T_1-weighted maps were acquired from the MOLLI sequence. Endocardial and epicardial contours were manually drawn on all slices of T_1-weighted maps obtained in the end-diastolic phase in the LV, and the T_1-weighted blood pool values were calculated based on the LV cavity drawn manually. The ECV_{MR} map was then generated automatically after entry of the Hct value into the software (*Figure 3A-3C*). Finally, polar maps were generated according to the AHA's 16-segment model, and the ECV_{MR} value of each segment was determined (*Figure 3D*). Myocardial ECV_{MR} (%) was calculated using the following equation (18):

$$ECV_{MR}=\frac{R1_{myocardium\ post}-R1_{myocardium\ pre}}{R1_{blood\ pool\ post}-R1_{blood\ pool\ pre}}\times(100-Hct) \quad [3]$$

where R1 is equal to 1/T1 value (T1 value of myocardial tissue was measured by T1-weighted mapping), $R1_{myocardium\ post}$ is 1/T1 value of myocardial tissue obtained after the contrast was injected, $R1_{myocardium\ pre}$ is 1/T1 value of myocardial tissue obtained before the contrast was injected, $R1_{blood\ pool\ post}$ is 1/T1 value of blood pool obtained after the contrast was injected, and $R1_{blood\ pre}$ is 1/T1 value of blood pool obtained before the contrast was injected.

Statistical analysis

Continuous variables were expressed as the mean ± SD, and those with a normal distribution were compared using paired *t*-tests. Categorical variables were expressed as numbers and percentages. Interobserver variability in the evaluation of ECV_{MR}, ECV_{CT}, and IQ was assessed using intraclass correlation coefficients (ICC). Correlations between ECV_{MR} and ECV_{CT} were tested using Pearson's correlation coefficient. Bland–Altman plots were used to analyze the consistency of ECV_{MR} and ECV_{CT}. Two-sided $P<0.05$ was considered statistically significant. Statistical analyses were performed using SPSS version 20.0 (IBM Corp., Armonk, NY, USA).

Results

Patient characteristics and IQ scores

A total of 21 patients with planned follow-up examinations

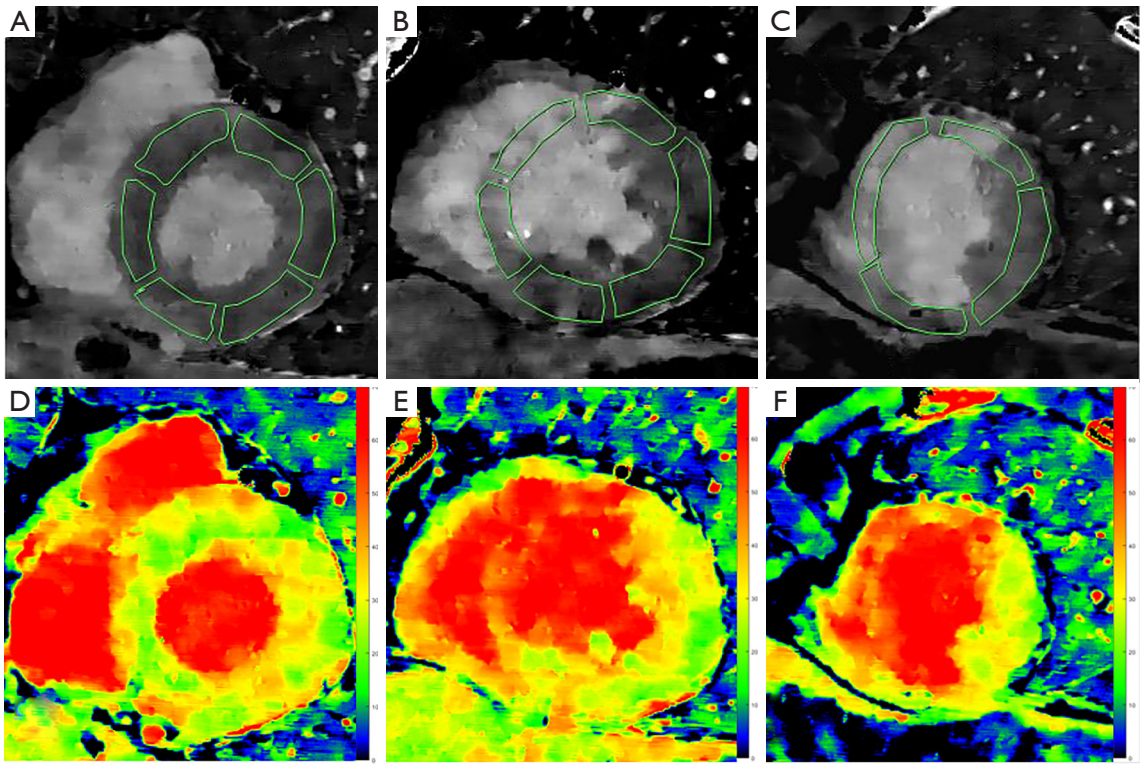

Figure 2 Measurement of myocardial ECV_{CT}, based on the AHA 16-segment model, in a patient (a 67-year-old man with inferior myocardial infarction) who underwent percutaneous coronary intervention. (A-C) Iodine maps obtained with delayed contrast-enhanced dual-layer spectral detector computed tomography. The regions of interest (green) are the areas for which ECV_{CT} was calculated based on AHA left ventricular segmentation. (D,E) Corresponding ECV_{CT} maps showing that ECV_{CT} values of the infarcted myocardium are higher (red). ECV_{CT}, extracellular volume quantified by computed tomography; AHA, American Heart Association.

3 months after PCI were enrolled in the present study; of them, 19 patients successfully completed cardiac CT and CMR scans, while two patients failed to undergo CMR scans because of arrhythmia. None of the 21 patients experienced an adverse event. There was good interobserver agreement in the scoring of IQ for CT and CMR images, with ICCs of 0.93 and 0.92, respectively. Sixteen patients with an IQ score ≥2 were enrolled in the final analysis (2 patients were excluded because of poor IQ caused by breathing artifacts on CMR images, and 1 patient was excluded because of a step artifact of the coronary arteries on CT images). The mean IQ scores for CT and CMR images were 3.81±0.40 and 3.25±0.58, respectively. Cardiovascular MR images were graded as excellent in 5 cases, good in 10, and moderate in 1, whereas CT images were graded as excellent in 13 cases and good in 3. The mean age of the 16 patients (13 males; 3 females) was 57.31±9.56 years. Detailed demographic characteristics are presented in *Table 1*.

Correlation analysis of ECVCT and ECVMR

According to the AHA's 16-segment model, 256 LV segments were analyzed, and the ECV_{CT} and ECV_{MR} values were calculated for each segment.

There was good interobserver agreement for ECV_{CT} (ICC =0.85) and ECV_{MR} (ICC =0.83).

The mean ECV_{CT} was 35.93%±9.73%, which was higher than the mean ECV_{MR} (33.89%±7.51%; P<0.01). There was a good correlation between ECV_{CT} and ECV_{MR} (r=0.79, P<0.001; *Figure 4*). The Bland–Altman plot showed a difference of 2.04% (95% CI: –9.56%, 13.64%) between the ECV_{CT} and ECV_{MR} values (*Figure 5*).

Discussion

In this study, the ECV of 256 myocardial segments in patients after PCI was calculated using both iodine and T_1-weighted mapping. There was good correlation between

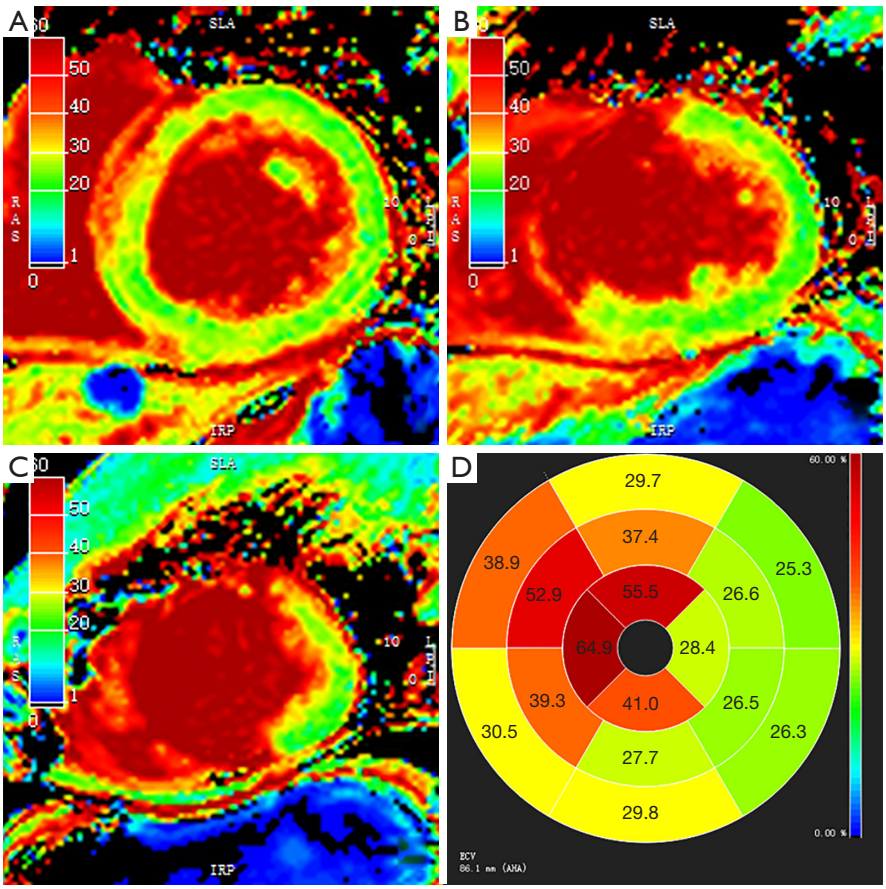

Figure 3 Measurement of myocardial ECV_{MR}, based on the AHA 16-segment model in the same patient as in *Figure 2*. (A-C) Extracellular volume mapping generated from cardiac magnetic resonance imaging showing higher ECV_{MR} values for the infarcted myocardium (red). (D) Polar mapping based on the AHA 16-segment model and ECV_{MR} values for each segment. The regions of infarcted myocardium shown by ECV_{CT} mapping are consistent with the those shown in the corresponding ECV_{MR} mapping. ECV_{MR}, extracellular volume quantified by cardiac magnetic resonance imaging; ECV_{CT}, extracellular volume quantified by computed tomography; AHA, American Heart Association.

ECV_{CT} and ECV_{MR}, with the mean difference being 2.04%.

Although the usefulness of ECV based on cardiac CT has been reported in patients with Takotsubo cardiomyopathy and cardiotoxicity (19,20), the present study is the first to use an iodine-based ECV method to evaluate myocardial status in patients after PCI. Like the gadolinium-containing contrast agent used in CMR, the iodine-containing contrast used in CT examinations could also be an extracellular tracer, and myocardial iodine concentrations in the equilibrium phase could be used to calculate ECV (18). Our results are in line with those of previous studies. In a comparative study of animal and human tissues, Jablonowski *et al.* (21) reported that ECV_{CT} could predict the degree of myocardial injury. These authors inferred that ECV_{CT} may detect microinfarctions caused by microembolization and segmental infarction caused by coronary artery occlusion (21). In a study that compared ECV_{CT} and ECV_{MR} between patients with heart failure and healthy volunteers, preliminary results indicated that there was a good correlation between ECV_{CT} and ECV_{MR} (8), and the method was optimized in follow-up study (8,9). The present study also found a good correlation between iodine-based ECV (ECV_{CT}) and ECV derived from CMR imaging (ECV_{MR}), with only a small difference observed between them. Therefore, for evaluating myocardial recovery in patients after PCI, iodine-based ECV from SDCT is a feasible substitution for CMR-derived ECV.

Currently, CMR imaging is a widely proposed non-invasive method for myocardial evaluation. However, CMR scans may fail, or the IQ may be affected by respiration

Table 1 Characteristics of the study population (n=16)

Variables	Data
Age (years)	57.31±9.56
Male sex	13 (81.25)
BMI (kg/m^2)	25.86±2.33
Hct (%)	40.63±4.67
Comorbidities	
Hypertension	13 (81.25)
Diabetes	15 (93.75)
Hyperlipidemia	14 (87.50)
Cerebral infarction	14 (87.50)
Location of lesions	
Inferior wall	13 (81.25)
Extensive anterior wall	2 (12.50)
Posterior wall	5 (31.25)
Preoperative myocardial markers	
Cardiac troponin T (U/L)	5.58±3.93
CK-MB (μg/mL)	231.12±156.06
Medication	
Aspirin	12 (75.00)
Clopidogrel	2 (12.50)
Statin	9 (56.25)
None	2 (12.50)
Stent type	
Firebird2 (MicroPort)	5 (31.25)
Firehawk (MicroPort)	3 (18.75)
Xience Prime (Abbott)	6 (37.50)
Endeavor Resolute (Medtronic)	2 (12.50)
Effective radiation dose (mSv)	3.61±0.45

Data presented as the mean ± SD or n (%). BMI, body mass index; Hct, hematocrit; CK-MB, creatine kinase isoenzyme-MB.

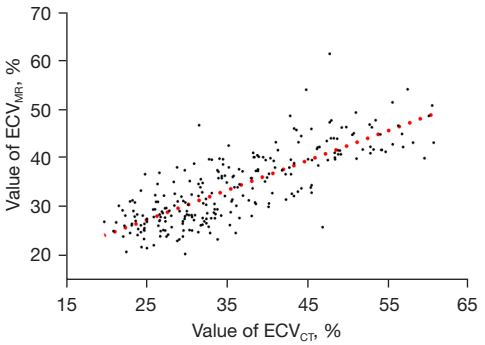

Figure 4 The correlation between ECV_{CT} and cardiac ECV_{MR} (r=0.79, P<0.001). ECV_{CT}, extracellular volume quantified by computed tomography; ECV_{MR}, extracellular volume quantified by cardiac magnetic resonance imaging.

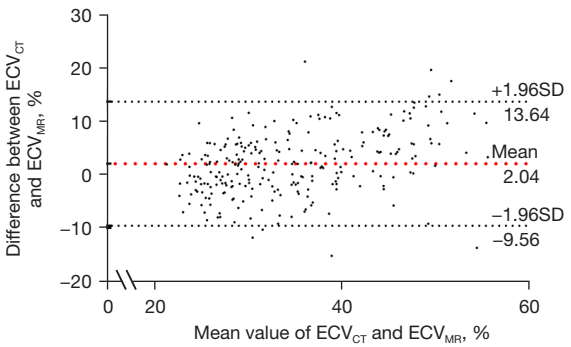

Figure 5 Bland–Altman plot comparing ECV_{CT} and that quantified by cardiac ECV_{MR}, showing a difference of 2.04% (95% CI: –9.56%, 13.64%). ECV_{CT}, extracellular volume quantified by computed tomography; ECV_{MR}, extracellular volume quantified by cardiac magnetic resonance imaging.

artifacts due to prolonged scanning. In the present study, CMR scans failed in 2 patients with arrhythmia, and another 2 patients were excluded because of poor IQ; however, all cardiac CT scans were completed successfully, and only 1 patient was excluded because of discontinuation of the coronary arteries. In contrast with ECV_{MR}, iodine-based ECV_{CT} only required additional LIE scans after standard CCTA scans, which could save time and costs for patients. Moreover, ECV_{MR} requires pre- and postcontrast enhancement scans, which may result in mage registration errors between the two phases. Thus, iodine-based ECV_{CT} could provide more accurate results and enable one-step cardiac coronary and myocardial evaluation in patients after PCI. Furthermore, ECV_{CT} obtained from SDCT, which benefits from a higher spatial resolution than MR (10,22,23), could improve the diagnostic confidence for small myocardial perfusion defects. The evaluation of IQ in this study showed that the IQ scores were significantly higher with CT than with CMR imaging. Furthermore, detector-based dual-energy CT had spatially and temporally matched high- and low-energy X-rays, allowing for projection-space

material decomposition, which is critical for cardiac spectral scans. Also, unlike with tube-based dual-energy CT, the on-demand retrospective spectra require no changes to the routine clinical workflow.

This study has several limitations that need to be considered. First, the myocardium was segmented manually on CT images, which may have resulted in error from patient to patient. However, the ICC results for ECV_{CT} indicated good agreement between the two radiologists. Second, artifacts caused by stents on CT images may also affect the measurement of iodine values, impacting on the accuracy of ECV_{CT}. Also, differences in the delay time after contrast injection for LIE may have also affected the result of this study. Although some studies on ECV have analyzed the time required to achieve stability after contrast injection (24-26), no study to date has suggested an optimal delay time; therefore, more studies are needed to clarify this issue. Third, although we analyzed the consistency of ECV_{CT} and ECV_{MR} from 256 LV segments, the sample size was still small.

Conclusions

Iodine-based ECV obtained by SDCT is highly correlated with ECV obtained from CMR imaging and could serve as a biomarker for myocardial evaluation. In combination with CCTA, SDCT could be used for one-step cardiac follow-up examination in patients after PCI.

Acknowledgments

The authors thank all the study investigators, clinicians, nurses, and technicians for dedicating their time and skills to the completion of this study.

Funding: This work was supported by the Natural Science Foundation of China (Nos. 92068116, 81870358), the Key Projects of Science and Technology of Jiangsu Province (No. BE2019602), the Science Fund for Distinguished Young Scholars in Jiangsu Province, the Innovation and Entrepreneurship Doctoral Foundation (No. JSSCBS20211534), the Nanjing Medical Science and Technique Development Foundation (Nos. ZKX19018, QRX17057), China Postdoctoral Science Foundation (No. 2019M661804), and Jiangsu Province Postdoctoral Science Foundation (No. 2019k060).

Footnote

Reporting Checklist: The authors have completed the STARD reporting checklist. Available at https://qims.amegroups.com/article/view/10.21037/qims-21-1103/rc

Conflicts of Interest: All authors have completed the ICMJE uniform disclosure form (available at https://qims.amegroups.com/article/view/10.21037/qims-21-1103/coif). ZS and XC are employees of Philips Healthcare. The other authors have no conflicts of interest to declare.

Ethical Statement: The authors are accountable for all aspects of the work and ensuring that questions related to the accuracy or integrity of any part of the work are appropriately investigated and resolved. The study was conducted in accordance with the Declaration of Helsinki (as revised in 2013). The study was approved by the Institutional Review Board of Nanjing Drum Tower Hospital (No. 2018-046-01), and written informed consent was obtained from all patients.

References

1. Rauch U, Osende JI, Fuster V, Badimon JJ, Fayad Z, Chesebro JH. Thrombus formation on atherosclerotic plaques: pathogenesis and clinical consequences. Ann Intern Med 2001;134:224-38.
2. Doenst T, Haverich A, Serruys P, Bonow RO, Kappetein P, Falk V, Velazquez E, Diegeler A, Sigusch H. PCI and CABG for Treating Stable Coronary Artery Disease: JACC Review Topic of the Week. J Am Coll Cardiol 2019;73:964-76.
3. Giannini F, Candilio L, Mitomo S, Ruparelia N, Chieffo A, Baldetti L, Ponticelli F, Latib A, Colombo A. A Practical Approach to the Management of Complications During Percutaneous Coronary Intervention. JACC Cardiovasc Interv 2018;11:1797-810.
4. Hammer-Hansen S, Bandettini WP, Hsu LY, Leung SW, Shanbhag S, Mancini C, Greve AM, Køber L, Thune JJ, Kellman P, Arai AE. Mechanisms for overestimating

acute myocardial infarct size with gadolinium-enhanced cardiovascular magnetic resonance imaging in humans: a quantitative and kinetic study. Eur Heart J Cardiovasc Imaging 2016;17:76-84.
5. Kidambi A, Motwani M, Uddin A, Ripley DP, McDiarmid AK, Swoboda PP, Broadbent DA, Musa TA, Erhayiem B, Leader J, Croisille P, Clarysse P, Greenwood JP, Plein S. Myocardial Extracellular Volume Estimation by CMR Predicts Functional Recovery Following Acute MI. JACC Cardiovasc Imaging 2017;10:989-99.
6. Bulluck H, Rosmini S, Abdel-Gadir A, White SK, Bhuva AN, Treibel TA, Fontana M, Gonzalez-Lopez E, Reant P, Ramlall M, Hamarneh A, Sirker A, Herrey AS, Manisty C, Yellon DM, Kellman P, Moon JC, Hausenloy DJ. Automated Extracellular Volume Fraction Mapping Provides Insights Into the Pathophysiology of Left Ventricular Remodeling Post-Reperfused ST-Elevation Myocardial Infarction. J Am Heart Assoc 2016;5:003555.
7. Schmermund A, Eckert J, Schmidt M, Magedanz A, Voigtländer T. Coronary computed tomography angiography: a method coming of age. Clin Res Cardiol 2018;107:40-8.
8. Nacif MS, Kawel N, Lee JJ, Chen X, Yao J, Zavodni A, Sibley CT, Lima JA, Liu S, Bluemke DA. Interstitial myocardial fibrosis assessed as extracellular volume fraction with low-radiation-dose cardiac CT. Radiology 2012;264:876-83.
9. Nacif MS, Liu Y, Yao J, Liu S, Sibley CT, Summers RM, Bluemke DA. 3D left ventricular extracellular volume fraction by low-radiation dose cardiac CT: assessment of interstitial myocardial fibrosis. J Cardiovasc Comput Tomogr 2013;7:51-7.
10. Wang X, Meier D, Taguchi K, Wagenaar DJ, Patt BE, Frey EC. Material separation in x-ray CT with energy resolved photon-counting detectors. Med Phys 2011;38:1534-46.
11. Everaars H, van der Hoeven NW, Janssens GN, van Leeuwen MA, van Loon RB, Schumacher SP, Demirkiran A, Hofman MBM, van der Geest RJ, van de Ven PM, Götte MJ, van Rossum AC, van Royen N, Nijveldt R. Cardiac Magnetic Resonance for Evaluating Nonculprit Lesions After Myocardial Infarction: Comparison With Fractional Flow Reserve. JACC Cardiovasc Imaging 2020;13:715-28.
12. Fukui M, Xu J, Abdelkarim I, Sharbaugh MS, Thoma FW, Althouse AD, Pedrizzetti G, Cavalcante JL. Global longitudinal strain assessment by computed tomography in severe aortic stenosis patients - Feasibility using feature tracking analysis. J Cardiovasc Comput Tomogr 2019;13:157-62.
13. Oda S, Emoto T, Nakaura T, Kidoh M, Utsunomiya D, Funama Y, Nagayama Y, Takashio S, Ueda M, Yamashita T, Tsujita K, Ando Y, Yamashita Y. Myocardial Late Iodine Enhancement and Extracellular Volume Quantification with Dual-Layer Spectral Detector Dual-Energy Cardiac CT. Radiol Cardiothorac Imaging 2019;1:e180003.
14. Qin L, Gu S, Chen C, Zhang H, Zhu Z, Chen X, Han Q, Yan F, Yang W. Initial exploration of coronary stent image subtraction using dual-layer spectral CT. Eur Radiol 2019;29:4239-48.
15. Ota H, Yarnykh VL, Ferguson MS, Underhill HR, Demarco JK, Zhu DC, Oikawa M, Dong L, Zhao X, Collar A, Hatsukami TS, Yuan C. Carotid intraplaque hemorrhage imaging at 3.0-T MR imaging: comparison of the diagnostic performance of three T1-weighted sequences. Radiology 2010;254:551-63.
16. Johnson TR, Krauss B, Sedlmair M, Grasruck M, Bruder H, Morhard D, Fink C, Weckbach S, Lenhard M, Schmidt B, Flohr T, Reiser MF, Becker CR. Material differentiation by dual energy CT: initial experience. Eur Radiol 2007;17:1510-7.
17. Lee HJ, Im DJ, Youn JC, Chang S, Suh YJ, Hong YJ, Kim YJ, Hur J, Choi BW. Myocardial Extracellular Volume Fraction with Dual-Energy Equilibrium Contrast-enhanced Cardiac CT in Nonischemic Cardiomyopathy: A Prospective Comparison with Cardiac MR Imaging. Radiology 2016;280:49-57.
18. Scully PR, Bastarrika G, Moon JC, Treibel TA. Myocardial Extracellular Volume Quantification by Cardiovascular Magnetic Resonance and Computed Tomography. Curr Cardiol Rep 2018;20:15.
19. Sueta D, Oda S, Yamamoto E, Nishi M, Kaikita K, Kidoh M, Utsunomiya D, Nakaura T, Yamashita Y, Tsujita K. Takotsubo Cardiomyopathy Mimicking Acute Coronary Syndrome - Extracellular Volume Quantification Using Cardiac Computed Tomography. Circ J 2019;83:1613.
20. Sueta D, Kidoh M, Oda S, Egashira K, Yamamoto E, Kaikita K, Matsushita K, Yamamoto Y, Hirai T, Tsujita K. Usefulness of Cardiac Computed Tomography in the Diagnosis of Anti-Cancer Therapy-Related Cardiac Dysfunction - Consistency With Magnetic Resonance Imaging. Circ J 2021;85:393-6.
21. Jablonowski R, Wilson MW, Do L, Hetts SW, Saeed M. Multidetector CT measurement of myocardial extracellular volume in acute patchy and contiguous infarction: validation with microscopic measurement.

Radiology 2015;274:370-8.
22. Chen MY, Rochitte CE, Arbab-Zadeh A, Dewey M, George RT, Miller JM, et al. Prognostic Value of Combined CT Angiography and Myocardial Perfusion Imaging versus Invasive Coronary Angiography and Nuclear Stress Perfusion Imaging in the Prediction of Major Adverse Cardiovascular Events: The CORE320 Multicenter Study. Radiology 2017;284:55-65.
23. Yamasaki Y, Abe K, Kamitani T, Sagiyama K, Hida T, Hosokawa K, Matsuura Y, Hioki K, Nagao M, Yabuuchi H, Ishigami K. Right Ventricular Extracellular Volume with Dual-Layer Spectral Detector CT: Value in Chronic Thromboembolic Pulmonary Hypertension. Radiology 2021;298:589-96.
24. Hong YJ, Kim TK, Hong D, Park CH, Yoo SJ, Wickum ME, Hur J, Lee HJ, Kim YJ, Suh YJ, Greiser A, Paek MY, Choi BW. Myocardial Characterization Using Dual-Energy CT in Doxorubicin-Induced DCM: Comparison With CMR T1-Mapping and Histology in a Rabbit Model. JACC Cardiovasc Imaging 2016;9:836-45.
25. Kawel N, Nacif M, Santini F, Liu S, Bremerich J, Arai AE, Bluemke DA. Partition coefficients for gadolinium chelates in the normal myocardium: comparison of gadopentetate dimeglumine and gadobenate dimeglumine. J Magn Reson Imaging 2012;36:733-7.
26. Lee JJ, Liu S, Nacif MS, Ugander M, Han J, Kawel N, Sibley CT, Kellman P, Arai AE, Bluemke DA. Myocardial T1 and extracellular volume fraction mapping at 3 tesla. J Cardiovasc Magn Reson 2011;13:75.

Cite this article as: Liang J, Li H, Xie J, Yu H, Chen W, Yin K, Chen X, Sheng Z, Zhang X, Mu D. Iodine-based extracellular volume for evaluating myocardial status in patients undergoing percutaneous coronary intervention for acute myocardial infarction by using dual-layer spectral detector computed tomography: a comparison study with magnetic resonance. Quant Imaging Med Surg 2022;12(9):4502-4511. doi: 10.21037/qims-21-1103

